AD-A050 311 BALLISTIC RESEARCH LABS ABERDEEN PROVING GROUND MD F/G 19/1
CONJECTURE FOR ANOMALOUS SPIN DECAY OF THE 155MM BINARY SHELL (--ETC(U)
OCT 77 C W KITCHENS, R SEDNEY

UNCLASSIFIED BRL-2026 NL

1 OF 1
AD A050311

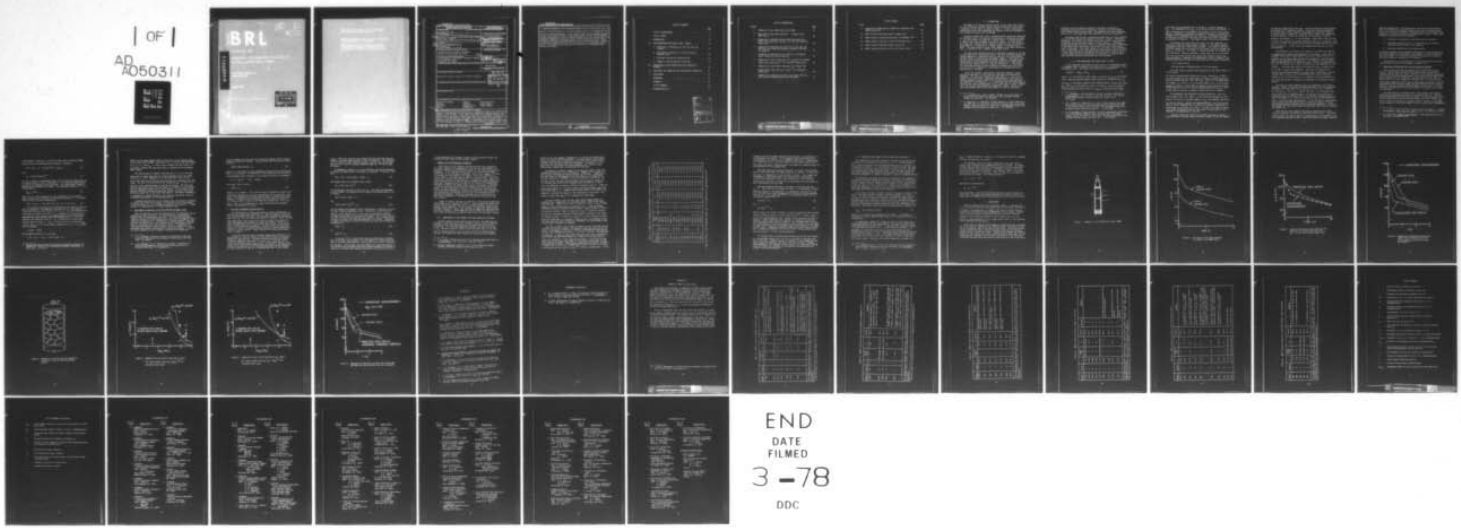

END
DATE FILMED
3-78
DDC

AD A050311

(12) 9

AD

BRL

REPORT NO. 2024

CONJECTURE FOR ANOMALOUS SPIN DECAY OF THE 155mm BASANT SHELL (XM449)

Charles H. Murphy, Jr.

DDC
RECEIVED
FEB 23 1978
B

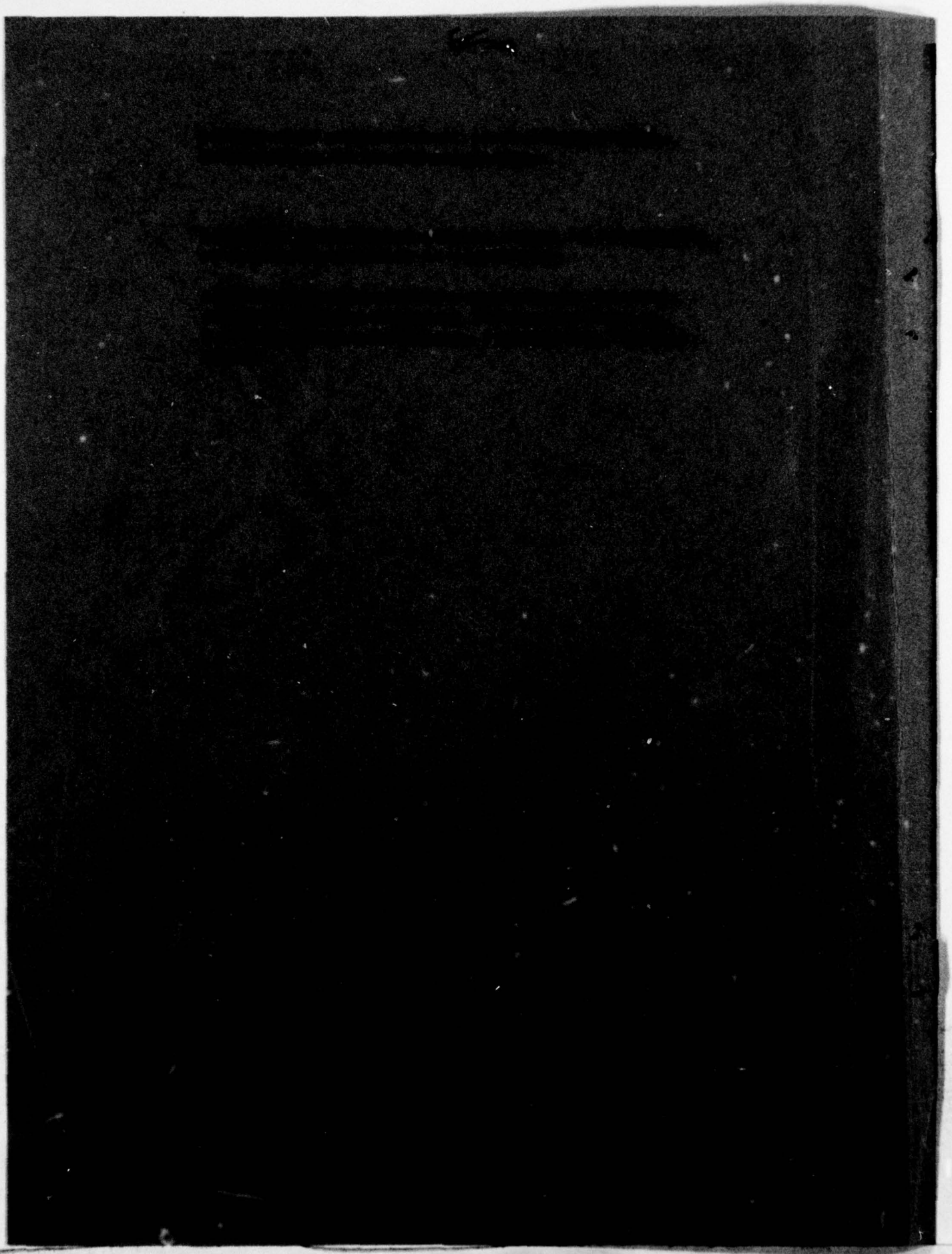

UNCLASSIFIED

SECURITY CLASSIFICATION OF THIS PAGE (When Data Entered)

REPORT DOCUMENTATION PAGE

READ INSTRUCTIONS BEFORE COMPLETING FORM

1. REPORT NUMBER: BRL REPORT NO. 2026
2. GOVT ACCESSION NO.
3. RECIPIENT'S CATALOG NUMBER

4. TITLE (and Subtitle): Conjecture for Anomalous Spin Decay of the 155mm Binary Shell (XM687).

5. TYPE OF REPORT & PERIOD COVERED: Final rept.

6. PERFORMING ORG. REPORT NUMBER: BRL-2026

7. AUTHOR(s): Clarence W. Kitchens, Jr.
Raymond Sedney

8. CONTRACT OR GRANT NUMBER(s): RDT&E 1W161102AH43

9. PERFORMING ORGANIZATION NAME AND ADDRESS: US Army Ballistic Research Laboratory
Aberdeen Proving Ground, MD 21005

10. PROGRAM ELEMENT, PROJECT, TASK AREA & WORK UNIT NUMBERS

11. CONTROLLING OFFICE NAME AND ADDRESS: US Army Materiel Development & Readiness Command
5001 Eisenhower Avenue
Alexandria, VA 22333

12. REPORT DATE: OCT 77

13. NUMBER OF PAGES: 50 (12) 41p.

14. MONITORING AGENCY NAME & ADDRESS (if different from Controlling Office)

15. SECURITY CLASS. (of this report): UNCLASSIFIED

15a. DECLASSIFICATION/DOWNGRADING SCHEDULE

16. DISTRIBUTION STATEMENT (of this Report)

Approved for public release; distribution unlimited.

DDC
RECEIVED
FEB 23 1978
B

17. DISTRIBUTION STATEMENT (of the abstract entered in Block 20, if different from Report)

18. SUPPLEMENTARY NOTES

19. KEY WORDS (Continue on reverse side if necessary and identify by block number)

Liquid-Filled Shell	Laminar	Toroidal Vortices
Spin-Up	Turbulent	Taylor Number
Spin Decay	Boundary Layer	Flight Dynamics
Corner	Instability	

20. ABSTRACT (Continue on reverse side if necessary and identify by block number)

When the XM687 liquid-filled projectile is launched with small yaw a smooth spin record is obtained which can be accurately predicted by theories based on the Wedemeyer spin-up model. A few rounds with large first maximum yaw have a different type of spin record exhibiting a rapid initial spin decay, followed by a corner, or discontinuity in slope. This type record cannot be predicted by theories based on the Wedemeyer model. An examination of firing data shows that the first maximum yaw angle, α_o, and the launch rotational Reynolds number, Re_o,

(continued)

DD FORM 1 JAN 73 1473 EDITION OF 1 NOV 65 IS OBSOLETE

UNCLASSIFIED

SECURITY CLASSIFICATION OF THIS PAGE (When Data Entered)

050 750

are important parameters which determine whether or not a corner exists; α_o is a measure of the perturbation to the liquid payload and Re_o is an indicator of the stability of the liquid motion. Three possible types of fluid dynamic instabilities are considered to explain the spin record with a corner; two are rejected leading to the conjecture that a nonlinear instability in the spin-up flow is the responsible mechanism. An analysis based on this instability gives a fairly successful criterion for deciding whether or not a corner will occur. A model, incorporating toroidal vortices in the spin-up flow, is developed and used to predict a spin-decay history which has the characteristics observed on the records with corners.

TABLE OF CONTENTS

ACCESSION for
NTIS White Section ✓
DDC Buff Section
UNANNOUNCED
JUSTIFICATION
BY
DISTRIBUTION/AVAILABILITY CODES
Dist. AVAIL. and/or SPECIAL
A

LIST OF ILLUSTRATIONS

PRECEDING PAGE BLANK-NOT FILMED

LIST OF TABLES

PRECEDING PAGE BLANK-NOT FILMED

I. INTRODUCTION

The XM687 is the binary payload carrier of the 155mm, M483, family. Its two cylindrical canisters contain fluids separated by burst discs. A schematic of this shell is shown in Figure 1. In-bore acceleration ruptures the burst discs permitting the liquids in the two canisters to mix by means of spin-up and by sloshing.

Firings of XM687 shell with a simulated binary agent have exhibited two different types of projectile spin histories, illustrated in Figure 2. The spin history for round 3A1, labeled Type S, is characterized by a "smooth" spin decay throughout the entire flight. The spin history for round 10G5, labeled Type C, exhibits a rapid initial spin decay for approximately 1-2s followed by a sudden change to a smaller rate of decay. The sharp change in slope, which appears to be almost discontinuous, is referred to as a "corner" in the spin record.

The Type S spin history has been conventionally observed in firings of spin-stabilized, liquid-filled shell. The spin decreases smoothly as angular momentum is transferred from the casing to the liquid payload and the casing is acted upon by aerodynamic moments. This kind of spin history can be accurately predicted using a numerical procedure which simultaneously solves Wedemeyer's spin-up equation for a 100%-filled canister and the projectile roll equation, Reference 1. Calculations for conditions similar to those of round 3A1 indicate that the liquid spin-up process is completed in approximately 19 seconds when Type S spin history is observed.

Type C spin history, observed for round 10G5, implies a liquid spin-up process which is very different from the one postulated by Wedemeyer. The spin loss incurred in round 10G5 by t = 1.4s, at the corner in the spin record, corresponds approximately to the amount of angular momentum transfer needed to fully spin-up the liquid payload; see Appendix B of Reference 2. It is surprising that the liquid spin-up time for this round, approximately 1.4s, is more than an order of magnitude shorter than that predicted by Wedemeyer's model. Figure 3 compares the measured spin history for round 10G5 with the spin decay

---

1. *C. W. Kitchens, Jr., and N. Gerber, "Prediction of Spin-Decay of Liquid-Filled Projectiles," BRL Report 1996, Aberdeen Proving Ground, MD, July 1977. (AD A043275)*

2. *V. Oskay and J. H. Whiteside, "Flight Behavior of 155mm (XM687 Mod I and XM687 Mod II) and 8-Inch (XM736 Mod I) Binary Shell at Nicolet, Canada, During the Winter of 1974-1975," BRL Memorandum Report 2608, Aberdeen Proving Ground, MD, March 1976. (AD B010566L)*

PRECEDING PAGE BLANK-NOT FILMED

predicted using the Wedemeyer model[3] as described in Reference 1, including in-bore effects and assuming a turbulent end-wall boundary layer, often called an Ekman layer. The measured spin decay during the first 1.4s is 70% larger than that predicted by the spin decay model.

The Type C spin history, obtained for round 10G5, was first noticed in the 1974-1975 winter test program at Nicolet, Canada[2]. Afterwards, examination of previous firing data[4] from tests at Yuma Proving Ground and Wallops Island provided a number of other examples. Subsequent firings during the 1975-1976 winter test program[5] showed that, depending on the shell launch conditions, either Type S or Type C spin history could be obtained. This report presents a correlation of the available data, a conjecture on the flow process occurring during spin-up for Type C rounds and a method for estimating their spin decay. These results are not completely successful and must be regarded as tentative until data from more carefully controlled tests are available.

II. FLOW MECHANISMS THAT MIGHT CAUSE A CORNER

In all equations the projectile spin rate, p, is expressed in units of radians/s, but in figures it has units of rev/s to correspond to the experimental data. Spin decay of a projectile is governed by

$$I_z dp/dt = - (M_{Aero} + M_{Liq}) \qquad (1)$$

where I_z is the projectile axial moment of inertia, M_{Aero} is the aerodynamic, spin-decelerating moment (characterized by the coefficient C_{ℓ_p}) and M_{Liq} is the moment exerted by the liquid payload. We must know both M_{Aero} and M_{Liq} as functions of p and t in order to be able to predict the projectile spin decay from (1). M_{Aero} is determined from flight

---

3. *E. H. Wedemeyer, "The Unsteady Flow Within a Spinning Cylinder," J. Fluid Mech., Vol. 10, Part 3, 1964, pp. 383-399. Also see BRL Report 1252, Aberdeen Proving Ground, MD, October 1963. (AD 431846)*

4. *W. P. D'Amico, V. Oskay and W. H. Clay, "Flight Tests of the 155mm XM687 Binary Projectile and Associated Design Modifications Prior to the Nicolet Winter Test 1974-1975," BRL Memorandum Report 2748, Aberdeen Proving Ground, MD, May 1977. (AD B019969L)*

5. *J. H. Whiteside, "Flight Behavior Test of 155mm XM687E1 and XM718E1 and 8-Inch XM650E4, PXR6231, XM711 and XM736 Shell at Nicolet, Canada, During the Winter of 1975-1976," BRL Memorandum Report 2732, Aberdeen Proving Ground, MD, March 1977. (AD B018149L)*

tests with a solid payload; early in flight it is small compared to M_{Liq}. The determination of M_{Liq} is the central part of the problem. It must be deduced from a knowledge of the internal, liquid motion during spin-up. Reference 1 presents two methods of solving (1), within the framework of the Wedemeyer model for spin-up[3], and demonstrates that one of them gives results for spin decay that agree with Type S yawsonde measurements to within 1%. (The other is only a little less accurate.)

Calculating spin decay from this theory, for the conditions of round 10G5, gives the results shown in Figure 3. The theory requires axisymmetric flow and a 100%-filled cylinder. The former is not well satisfied because yaw was induced for this round, the first maximum yaw angle, α_o, being 8.8°. The latter is violated because the cylinder was only 87% filled. However, Reference 1 shows that, for α_o on the order of 4° and fill ratios of 90%, the theory still predicts Type S spin decay accurately. Compared to the theoretical result in Figure 3, the yawsonde measurement of spin for round 10G5 has 3 distinctive features:

(i) A corner exists,

(ii) The slope is constant from t = 0 to the corner,

(iii) The slope is greater than that given by the theory from t = 0 to the corner.

The slope is proportional essentially to M_{Liq}, since M_{Aero} is small. The third feature has also been found[1] for Type S cases for partially-filled cylinders and $Re_o \sim 10^6$, where $Re_o = p_o a^2/\nu$ is the launch Reynolds number, $p_o = p(0)$, a is the cylinder radius, and ν is the liquid kinematic viscosity. Since there is nothing in the theory that would permit features (i) and (ii) and the implied behavior of M_{Liq}, a different model of spin-up is needed to explain the Type C records.

The parameters that determine the spin history are: Re_o; the cavity aspect ratio, c/a, where c is the cavity half-height; α_o; the cavity fill ratio, β; the Mach number, M; C_{ℓ_p}; the quadrant elevation; and the air density, suitably non-dimensionalized. One of our conclusions is that a combination of α_o and Re_o is probably significant in determining the existence of a corner. To reduce the number of parameters being considered we discuss two rounds for which most of the parameters are approximately the same.

Yawsonde results for rounds 3A1 and 10G5 are shown in Figure 2. Both were fired in winter tests at Nicolet, Canada, so the air density

was high and approximately the same. They were launched from the M109A1 SP Howitzer at 30° quadrant elevation. Both shell were approximately 87% filled with a binary simulant consisting of a mixture of Freon 113 and ethyl alcohol. Round 3A1[5], with the Type S record, was launched at a muzzle velocity of 295.4 m/s so that M = 0.94 and $Re_o = 8.2\times10^5$. Without a yaw inducer, $\alpha_o = 2°$ was obtained. Round 10G5[2], with the Type C record, was launched at a muzzle velocity of 314.3 m/s so that M = 0.99 and $Re_o = 8.7\times10^5$; the higher velocity gives the higher initial spin rate shown in Figure 2. In this case a yaw inducer was used and $\alpha_o = 8.8°$ was obtained.

The differences in M and Re_o for rounds 3A1 and 10G5 are judged to be insignificant, apropos the appearance of the corner. Since the only parameter that differs significantly is α_o we can conclude that it is important to the corner question and that it provides a clue for determining a flow mechanism that causes it. In Section III all available data are examined and it is shown that Type C records are obtained only for $\alpha_o \geq 4°$, whereas Type S occur for smaller α_o, but sometimes also for larger α_o. Two other data points with about the same α_o indicate that Re_o is also a significant parameter. There are not enough data to isolate the remaining parameters and judge their significance. Thus we conclude that α_o and Re_o are two parameters whose values determine whether or not a corner exists; α_o is a measure of the perturbation to the liquid motion and, in general, Re_o indicates the stability of this motion.

There may be other parameters which are important to the corner question. Figure 4 shows the yawsonde measurements for two rounds with essentially the same values of α_o and Re_o; $\alpha_o = 8.3°$, $Re_o = 8.65\times10^5$ for 10G4 and $\alpha_o = 8.8°$, $Re_o = 8.68\times10^5$ for 10G5. The calculated spin decay curve will be discussed later. The initial slopes of the two records in Figure 4 differ by 50%; it is difficult to imagine that the small differences in α_o and Re_o can account for the large difference in slope. Two conclusions seem possible: (1) the firings are reproducible only to within the differences shown for these two rounds, or (2) an unidentified parameter accounts for the observed differences. There is some support for the second conclusion when some other data are examined, see Section III.

When the projectile emerges from the gun some fraction of the liquid is spinning; the amount is inversely related to Re_o. The launch process and/or yaw inducer imparts a perturbation to the projectile; the only observable measure of this is the first maximum yaw angle, obtained

from the yawsonde data. The question is: how will this perturbation affect the motion of the liquid; specifically, will it cause an instability in this motion leading to a spin-up process quite different from Wedemeyer's and thus an observed spin record with a corner? Three types of possible instabilities are considered:

A. Transition to turbulence in the flow near the side wall,

B. Centrifugal instability; i.e., Taylor vortices in the perturbation boundary layer at the sidewall,

C. Non-linear instability in the spin-up flow.

In making estimates of the parameters appropriate to these instabilities we use the Wedemeyer spin-up model, even though it is not accurate for the corner cases. It is the only available flow model and it should provide satisfactory estimates for our purposes.

The reader who is not interested in a detailed discussion of these instabilities can turn to the summary in Section II.D.

A. Transition to Turbulence in the Flow Near the Sidewall

Data on transition Reynolds numbers are available from experiments[6,7], mostly using two concentric cylinders with the outer one rotating and the inner one fixed. Reference 7 also presents calculated values of the critical Reynolds number as a function of the width of the gap, $\bar{S}$, between the two cylinders; it varies from 6×10^4 to 3×10^5 for $0.025 \leq \bar{S}/a \leq 1.0$. For rounds 10G4 and 10G5, $Re_o = 8.7\times10^5$, which is large enough compared to 3×10^5 that we might expect transition. But the calculated critical Reynolds number has uncertainties and the relation between it and the transition Reynolds number is not clear. If we consider the disturbance due to the yaw inducer, the balance tips in favor of transition.

The implications of turbulent flow at the sidewall were investigated and the resulting spin decay was calculated from (1). Taylor's torque measurements[6] for concentric cylinders, with the inner one fixed and the outer one rotating at constant speed, were used to obtain M_{Liq}; thus we treat the spin-up flow as quasi-steady. The gap, $\bar{S}$, was taken as the distance, D, from the sidewall to the inviscid front in Wedemeyer's

---

6. *G. I. Taylor, "Fluid Friction between Rotating Cylinders, I - Torque Measurements," Proc. Roy. Soc. London A, Vol. 157, 1936, pp. 546-564.*

7. *H. Schlichting, Boundary Layer Theory, p. 428, McGraw-Hill Book Co., New York, 4th Edition, 1960.*

spin-up model. Since $Re_o = 8.7\times10^5$ we expect that the endwall Ekman layers will be at least partially turbulent. Therefore

$$D(t) = a[1 - (1 + 0.6k_t pt)^{-5/3}] = ak_t pt + \ldots \quad , \tag{2}$$

with

$$k_t = 0.035\ (a/c)Re_o^{-1/5} \quad . \tag{3}$$

Eq. (2) is based on the Wedemeyer model with a turbulent Ekman layer and is derived from Eq. (8-58) of Reference 8. The indicated approximation for small t is adequate for our purposes. The instantaneous Reynolds number and $\bar{S}/a$ determine the torque. The aerodynamic moment in (1) can be expressed as

$$M_{Aero} = pf(t) \quad , \tag{4}$$

where f(t) is a known function of time, depending on the projectile shape, velocity and trajectory as described in Reference 1. For rounds 10G4 and 10G5 f(t) can be expressed as

$$f(t) = (1.25\ t - 13.5)\times10^{-4}\ kg - m^2/s \quad \text{for} \quad 0 \leq t \leq 3s \quad . \tag{5}$$

In the spin-decay calculation described here the torque on the endwalls is neglected. The numerical integration of (1) uses Taylor's torque data for M_{Liq} from launch up to $t = t_c$, $p = p_c$, the theoretically determined position of the corner; p_c is defined to be the projectile spin when the liquid reaches solid-body rotation and t_c is the corresponding time calculated from (1). p_c is determined by calculating angular momentum using (1). M_{Aero} is neglected and we substitute $M_{Liq} = dL/dt$, where L is the liquid angular momentum and $L(0) = 0$ is assumed. Thus (1) becomes

$$I_z\ dp/dt = -dL/dt$$

and integrating from 0 to t_c we obtain

$$I_z\ (p_c - p_o) = -L(t_c) = -\pi\rho ca^4\ p_c\beta(2 - \beta) \quad ;$$

---

8. *Engineering Design Handbook, Liquid-Filled Projectile Design, AMC Pamphlet No. 706-165, U.S. Army Materiel Command, Washington, DC, April 1969. (AD 853719)*

where ρ is the liquid density and β is the ratio of the liquid volume to the total cavity volume. The result is $p_c = 0.949\ p_o$ for both rounds. For $t \geq t_c$ we set $M_{Liq} = 0$ since we have assumed that the fluid is in solid-body rotation; the spin decay then is caused only by the aerodynamic torque.

The results given in Figure 4 show that for $0 \leq t \leq t_c$, the spin decay rate is larger than that for either yawsonde record; the corner occurs at $t_c = 0.4$s compared to 0.7s for round 10G4 and 1.4s for round 10G5; after the corner the three results have essentially the same slope. The last of these justifies the assumption $M_{Liq} = 0$ for $t \geq t_c$ and part of the assumed method of locating the corner. The first two results quoted above show that transition to turbulence on the sidewall does not adequately predict Type C spin records. If the torque on the endwalls had been included the predicted initial spin decay rate would have been larger and t_c would have been smaller. Therefore, although it is reasonable to assume transition, the predicted spin decay is not an acceptable approximation to the measured result.

Although turbulent flow at the sidewall does not provide a mechanism to explain the record with a corner, it indicates a way of decreasing the spin-up time; i.e., by inducing transition on the sidewall. A rough sidewall or protuberances on it might accomplish this.

B. Centrifugal Instability in the Perturbation Boundary Layer

When the spin-up or solid body rotation flows are perturbed, say by imparting an angle of attack, α, to the projectile, a perturbation boundary layer is induced near the walls. For solid-body rotation a linearized analysis of this boundary layer was given by Wedemeyer[9] and a numerical description of it, described in a separate report[10], has been obtained for spin-up flow. The thickness of the perturbation boundary layer is essentially the same for the two flows. In Reference 8 a centrifugal instability in this boundary layer was assumed to be the mechanism which caused a discontinuity in gyroscope records. A form of the Taylor number was used to deduce a criterion for instability,

---

9. *E. H. Wedemeyer, "Viscous Correction to Stewartson's Stability Criterion," BRL Report 1325, Aberdeen Proving Ground, MD, June 1966. (AD 489687)*

10. *C. W. Kitchens, Jr., N. Gerber and R. Sedney, "Calculation of Liquid Eigenfrequencies and Decay Rates during Spin-Up in a Cylinder," BRL Report (in preparation).*

tacitly assuming that the onset of instability depends on the relative velocity of the two cylinders. Their criterion for the onset of instability is

$$(a\bar{S}p/\nu)^2(\bar{S}/a)(\Delta V/ap) > C_1 \qquad (6)$$

where ΔV is the change in liquid tangential velocity across the gap, $\bar{S}$, and C_1 is a constant. In Reference 8, $\bar{S}$ was identified with the perturbation boundary-layer thickness, d, and from the results of Reference 9

$$\bar{S} = d = aRe_o^{-\frac{1}{2}} \quad \text{and} \quad \Delta V \propto ap\alpha \qquad (7)$$

were used. Then (6) gives

$$\alpha Re_o^{\frac{1}{2}} > C_2 \quad , \qquad (8)$$

where C_2 is a constant. This criterion can be regarded as a guide even though the conditions for Taylor's experiments are not satisfied. However, if the parameters for round 10G5 are used to estimate the Taylor number, it is found to be less than the critical value by a factor of 10. This is true, in spite of the large Re_o, because $d/a = 10^{-3}$ is so small. Thus it is unreasonable to assume the perturbation boundary layer to be unstable in our case.

C. Nonlinear Instability During Spin-Up

The spin-up flow is stable with respect to small disturbances, as shown by our calculations, Reference 10. Inviscid stability also follows from Rayleigh's criterion. For the large disturbances considered here (e.g., $\alpha_o \sim 8°$) the spin-up flow might be unstable. There are some well-known flows, such as pipe flow, that are stable with respect to small disturbances but unstable to large disturbances. There is no direct evidence that this is true for the spin-up flow; we conjecture that it is and seek the consequences. We also assume that the instability will result in toroidal vortices adjacent to the cylinder wall, similar to Taylor vortices. These vortices are illustrated schematically in Figure 5.

In the spin-up flow there is another length scale besides d, viz., the distance, D, from the sidewall to the inviscid front, as given in Wedemeyer's spin-up model. The main difference between the toriodal vortices assumed here and those in Section II.B is in their scale. Except for extremely small times, D will be much larger than d. The large scale of the vortices assumed here, see Figure 5, can enhance the mixing of the spinning with the non-spinning liquid and thus decrease the time required for spin-up, as observed when Type C spin records

occur. Since such vortices also increase the skin friction along the sidewall, the more rapid decrease in spin is plausible. The criterion, (6), is based on linear stability analysis, but for lack of any other guide we use it for our assumed nonlinear stability. We take $\Delta V \propto ap\alpha$ as before.

In Wedemeyer's model D(t) has two different expressions depending on whether the Ekman layers are laminar or turbulent. We take $\hat{S} = D(t)$ with

$$D(t) = a[1 - \exp(-k_\ell pt)] = ak_\ell pt + \ldots \tag{9}$$

for laminar flow[3] in the Ekman layers, where,

$$k_\ell = 0.443\,(a/c)\,Re_o^{-\frac{1}{2}} \quad . \tag{10}$$

In the turbulent case D(t) is given by (2). The indicated approximations for small t are adequate for our purposes and using these in (6) we obtain

$$(a/c)^3\,(pt)^3 \propto Re_o^{\frac{1}{2}} > C_3 \tag{11}$$

and

$$(a/c)^3\,(pt)^3 \propto Re_o^{7/5} > C_4 \tag{12}$$

for the laminar and turbulent cases, respectively. Criterion (11) has the same α and Re_o dependence as (8). The effect of the a/c and pt factors on the criteria (11) or (12) cannot be determined from the available data because a/c is relatively constant for all the data and the time of onset of the instability is unknown. Type C records show a constant spin decay rate from the beginning of the record. Henceforth we ignore the presence of these two factors and write the criterion for instability as

$$\alpha Re_o^{\frac{1}{2}} > C_5 \tag{13}$$

or

$$\alpha Re_o^{7/5} > C_6 \quad . \tag{14}$$

In Section III it is shown that these can successfully correlate most of the data, with respect to the occurrence of a corner; and also that a criterion involving only α_o and Re_o may not be able to correlate all the data. This success, plus the results of a spin decay calculation based on the flow model and torque formula presented in Section IV, leads us to conclude that nonlinear instability of the spin-up flow is

a likely mechanism for causing a corner in the spin-decay record; its conjectural basis must be kept in mind, however.

D. Summary of Flow Mechanisms Considered

Three types of fluid dynamic instabilities have been considered. The first, transition to turbulence in the flow near the sidewall, is plausible; however, the predicted spin decay is too large to accept this mechanism. It is ruled out on this basis. The second, centrifugal instability in the perturbation boundary layer at the sidewall, is ruled out because the flow appears to be stable. The Taylor number for a typical XM687 is ten times smaller than the critical value. The third, a nonlinear instability during spin-up, is conjectural since there is no direct evidence that the spin-up flow is unstable to large disturbances. Additional assumptions give (13) and (14) as criteria for instability, depending on whether the endwall Ekman layers are laminar or turbulent. It will be shown that these criteria correlate most of the data with respect to the occurrence of a corner. The flow model and torque for this conjectured instability, discussed in Section IV, give a predicted spin decay which is reasonably close to the value obtained from the yawsonde measurements. Therefore, nonlinear spin-up instability is a more likely candidate for the mechanism causing the spin record type with a corner.

A paper by Busse[11] that may be pertinent to the present problem has been brought to our attention by Scott[12]. Busse studied the steady flow inside a precessing spheroidal shell, including nonlinear terms in the boundary layer equations. Scott's analysis of that work indicates that nonlinear effects for large α may introduce an additional spin-up mechanism for a cylinder. If the magnitude of this effect is sufficient, it could offer an explanation, based on stable flow, for the Type C record.

III. CORRELATION OF SPIN RECORD TYPE WITH INSTABILITY CRITERIA

We have examined the available firing data for the XM687 shell to determine if the spin record type (smooth or corner) can be correlated with the criteria characterizing the conjectured nonlinear spin-up instability. In using the instability criteria (13) and (14) we take $\alpha = \alpha_o$. We expect critical values of the left hand sides of (13) and (14) to indicate whether or not toroidal vortices are formed during spin-up. For values less than critical the spin-up process should be

---

11. *F. H. Busse, "Steady Fluid Flow in a Precessing Spheroidal Shell," J. Fluid Mech., Vol. 33, Part 4, 1968, pp. 739-751.*

12. *Private communication from Dr. W. E. Scott, Launch and Flight Division, Ballistic Research Laboratory, June 1977.*

similar to the one assumed by Wedemeyer[3]; no vortices are formed and a Type S spin record would be obtained. For values larger than critical, toroidal vortices may be formed and the spin-up process would be much different than the one postulated by Wedemeyer. In Section IV it is shown that our conjecture plus some assumptions will lead to a spin record with a corner that is consistent with the data.

The Appendix contains a summary of the pertinent XM687 flight data examined for purposes of this correlation. Comments are included for some rounds to distinguish unusual features of the data. Inspection of the five tables in the Appendix shows that there are 17 rounds where data are available to determine α_o, Re_o and the spin record type. One of these rounds, 3B5, has canisters which are not keyed to the projectile casing; this round is not included in our correlation. Table 1 lists the remaining 16 rounds in order of increasing $\alpha_o(Re_o)^{\frac{1}{2}}$. There are seven rounds where a (?) is used to denote uncertainty about either the spin record type or α_o. Comments about these rounds are included in the Appendix to describe the nature of the uncertainty in each case. The values of $\alpha_o Re_o^{\frac{1}{2}}$ and $\alpha_o Re_o^{7/5}$ are tabulated for each round.

The two criteria, (13) and (14), come from assuming laminar or turbulent flow, respectively, in the Ekman layers. They do not apply simultaneously. Except for the first 3 entries in Table 1, Re_o is large enough so that we should have the turbulent case. In the following discussion, however, we present both criteria. From the data in Table 1, we find that critical values of $\alpha_o Re_o^{\frac{1}{2}}$ and $\alpha_o Re_o^{7/5}$ cannot be selected which give an absolute demarcation between Type S and Type C spin decay. The choices $\alpha_o(Re_o)^{\frac{1}{2}} = 4.5\times10^3$ or $\alpha_o(Re_o)^{7/5} = 9.2\times10^8$ furnish the lower bound for which Type C is observed. Theoretically, for parameter values less than critical, Type S records are obtained; for values greater than critical Type C records are obtained.

The data in Table 1 are plotted in Figure 6; Type S are open circles and Type C are filled circles. The critical values are shown by the two curves. The numbers 4.5×10^3 and 9.2×10^8 are determined by requiring the curves to pass through the point $\alpha_o = 5.1°$, $Re_o = 7.91\times10^5$, corresponding to round 4A1. A flag on a data point indicates there was an uncertainty about either the spin record type or α_o; these are the seven entries with a (?) in Table 1. First consider all points. To the left of each curve only Type S points are found. To the right of each curve all the Type C points are found. These results comply with the theory. However, 4 flagged Type S points or 5 flagged Type S points are also to the right of the curves for the $\alpha_o Re_o^{\frac{1}{2}}$ or $\alpha_o Re_o^{7/5}$ criterion, respectively. If the

Table 1. Comparison of Magnitude of Instability Parameters for XM687 Projectile

Round	β	Record Type	α_o	Re_o	$\alpha_o (Re_o)^{1/2}$	$\alpha_o (Re_o)^{7/5}$
7677	0.90	Smooth	1°	3.42×10^3	5.8×10^1	8.9×10^4
7670	1.00	Smooth	2.3°	3.32×10^3	1.3×10^2	2.0×10^5
7673	0.90	Smooth	3.1°	3.42×10^3	1.8×10^2	2.7×10^5
3A1	0.87	Smooth	2°	8.16×10^5	1.8×10^3	3.8×10^8
3644	*	Smooth (?)	2°	2.84×10^6	3.4×10^3	2.2×10^9
4A1	0.87	Corner	5.1°	7.91×10^5	4.5×10^3	9.2×10^8
7676	0.90	Smooth	4° (?)	1.70×10^6	5.2×10^3	2.1×10^9
5B1	0.87	Corner (?)	4°	1.83×10^6	5.4×10^3	2.3×10^9
7182	*	Corner	4.1°	2.94×10^6	7.0×10^3	4.7×10^9
10G4	0.87	Corner	8.3°	8.65×10^5	7.7×10^3	1.7×10^9
10G5	0.87	Corner	8.8°	8.68×10^5	8.2×10^3	1.8×10^9
7253	*	Corner	5.1°	2.96×10^6	8.8×10^3	5.9×10^9
7168	*	Smooth (?)	5.5°	2.89×10^6	9.4×10^3	6.1×10^9
7178	*	Smooth (?)	6.6°	2.81×10^6	1.1×10^4	7.0×10^9
3B2	0.87	Corner (?)	14.5°	8.13×10^5	1.3×10^4	2.7×10^9
3639	*	Smooth (?)	8.5°	2.80×10^6	1.4×10^4	9.0×10^9

* The fill ratio is not accurately known, but it is expected to be approximately 0.90.

flagged points are weighted equally with the others, the correlation is only moderately successful. If the flagged points are omitted from consideration, the correlation is completely successful. Perhaps there is a broand band of α_o, Re_o values above critical where either type of spin decay can occur; a definite conclusion cannot be reached because of the uncertainty of the flagged data.

Note that there are two pairs of points, one Type C and the other Type S, which have almost the same values for α_o and Re_o. In each case the Type S is flagged and in one the Type C is also. If we ignore the uncertainty in these three points, we would have to conclude that a criterion for separating types C and S, based solely on α_o and Re_o, could not be successful. Because of the uncertainty this conclusion is only a possibility, at this time.

The data indicate that Type C spin decay is observed only when $\alpha_o \geq 4°$. Since the shell yaw angle is large, it is reasonable to expect nonlinear effects to be important. The instability criteria (13) and (14) are based on a linear assumption for the form of the perturbation velocity, ΔV. To account, empirically, for nonlinear effects in α we arbitrarily changed these to

$$\alpha_o^2 \, (Re_o)^{1/2} > C_7 \tag{15}$$

and

$$\alpha_o^2 \, (Re_o)^{7/5} > C_8 \quad . \tag{16}$$

These criteria are tested in Figure 7; curves are shown for the selected critical values $\alpha_o^2 \, (Re_o)^{1/2} = 2.2\times10^4$ and $\alpha_o^2 \, (Re_o)^{7/5} = 4.7\times10^9$, chosen to give the lower bound for Type C points, as was done with the data in Figure 6. These correlations are, perhaps, a little more successful than the previous ones shown in Figure 6. All unflagged Type S points lie to the left of the two curves and all Type C points lie to the right. For each correlation, one less flagged Type S point appears to the right of each curve. A completely empirical approach could be tried to determine a separating boundary; for the data we have, nothing better than the curve $\alpha_o^2 \, Re_o^{1/2} = 2.2\times10^4$ could be expected.

We conclude that our correlations involving α_o and Re_o are successful in determing whether Type S or Type C spin decay is obtained, for most of the data. Complete success is achieved if the flagged data are omitted from consideration, but this is not yet justified. Perhaps other parameters, not measured in these tests; e.g., the initial yawing rate, will have to be included in the analysis to develop more successful correlating parameters.

IV. FLOW MODEL AND TORQUE FOR THE CONJECTURED INSTABILITY

The hypothesized nonlinear instability during spin-up must be supplemented by a flow model to estimate M_{Liq} in (1). We have assumed that a stack of toroidal vortices appears adjacent to the sidewall, as illustrated in Figure 5; i.e., the flow has a cellular form. The scale of these vortices in the radial direction is taken to be D(t) and they are assumed to have about the same height. The flow model yields the functional dependence of torque on the parameters of the problem; an additional assumption is needed to evaluate a constant of proportionality.

We appropriate the model described by Batchelor in the Appendix to Reference 13 for flow between two concentric cylinders, the outer fixed and the inner rotating at speeds well above the critical. He assumed steady, cellular flow and estimated the thickness of the boundary layer around the inviscid core of each vortex. Having this thickness, the functional dependence of torque on the gap width, angular velocity, and other pertinent quantities was easily obtained.

In our flow, the outer cylinder rotates with angular velocity p but there is no inner cylinder. Rather, the inner boundary is a shear layer: the front in the inviscid form of the Wedemeyer model of spin-up, which is at a distance D(t) from the cylinder. The shear layer boundary would give a different contribution to the estimate of boundary-layer thickness than the inner cylinder in Batchelor's case, but, for the order of magnitude estimates considered here, the difference can be neglected. The torque can be expressed, using Batchelor's analysis as

$$M_{Liq} = K(2c)a^4\rho p^2 Re_o^{-\frac{1}{2}}(a/D)^{\frac{1}{4}} \qquad (17)$$

where K is a constant not determined by the model. For laminar or turbulent flow in the endwall Ekman layer, D(t) is given by (9) or (2), respectively.

An additional assumption is needed to obtain K since there are no torque measurements for our configuration. We assume it can be estimated from rotating cylinder data. We used the data of Wendt in Figure 10 of Reference 13 since it extends to the large Re_o required. The parameters of round 10G5 were used to obtain the torque with D(t) obtained from (2) with t = 0.5s. Substituting these parameters and this torque into (17) gives K = 1.44. To estimate spin decay we calculate M_{Liq} from (17) with this K and then integrate (1) for all times up to the corner, which is located in the manner explained in Section II.A.

---

13. *R. J. Donnelly and N. J. Simon, "An Empirical Torque Relation for Supercritical Flow Between Rotating Cylinders," J. Fluid Mech., Vol. 7, Part 3, 1960, pp. 401-418.*

M_{Aero} is obtained from (4), using (5). The numerical result is compared with the yawsonde data in Figure 8.

The agreement with the yawsonde measurements for round 10G4 is rather close, considering the tenuous nature of our theory. No theory of this type can agree with both records because they have essentially the same observed flight parameters. Although the slope of the calculated spin decay curve in Figure 8 is not constant, from t = 0 to the corner, the curvature is not large. Using (1) and (17) an estimate of the variation of p with t can be made for small t:

$$p_o^{2.3} - p^{2.3} \sim t^{3/4}$$

from which an approximation

$$p_o - p \sim t^{3/4}$$

can be obtained. This shows the deviation from a linear variation for small time. The proper conclusion from this calculation is that our conjecture and assumptions are not contradicted by the firing test data.

V. CONCLUSIONS

When the 155mm liquid-filled projectile, XM687, is launched with $\alpha_o \geq 4°$ the spin record can show a rapid initial spin decay, followed by a "corner", or discontinuity in slope. This kind of record cannot be predicted by the theories based on Wedemeyer's spin-up model. Examination of the firing data revealed that α_o and Re_o are two important parameters which determine whether or not a corner exists; α_o is a measure of the perturbation to the liquid motion and Re_o is an indicator of the stability of this motion.

Three types of possible fluid dynamic instabilities were considered. Two were ruled out, leading to the conjecture that a nonlinear instability in the spin-up flow is the cause of the corner. The analysis based on this instability gives a fairly successful criterion for deciding whether or not a corner will occur. A model which incorporates toroidal vortices in the spin-up flow gives a calculated spin decay which has the characteristics observed on the records with corners. Thus far deductions from the conjecture and model are consistent with the firing data.

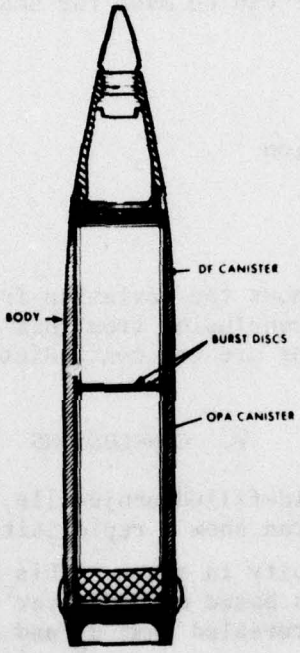

Figure 1. Schematic of the 155mm Binary Shell XM687

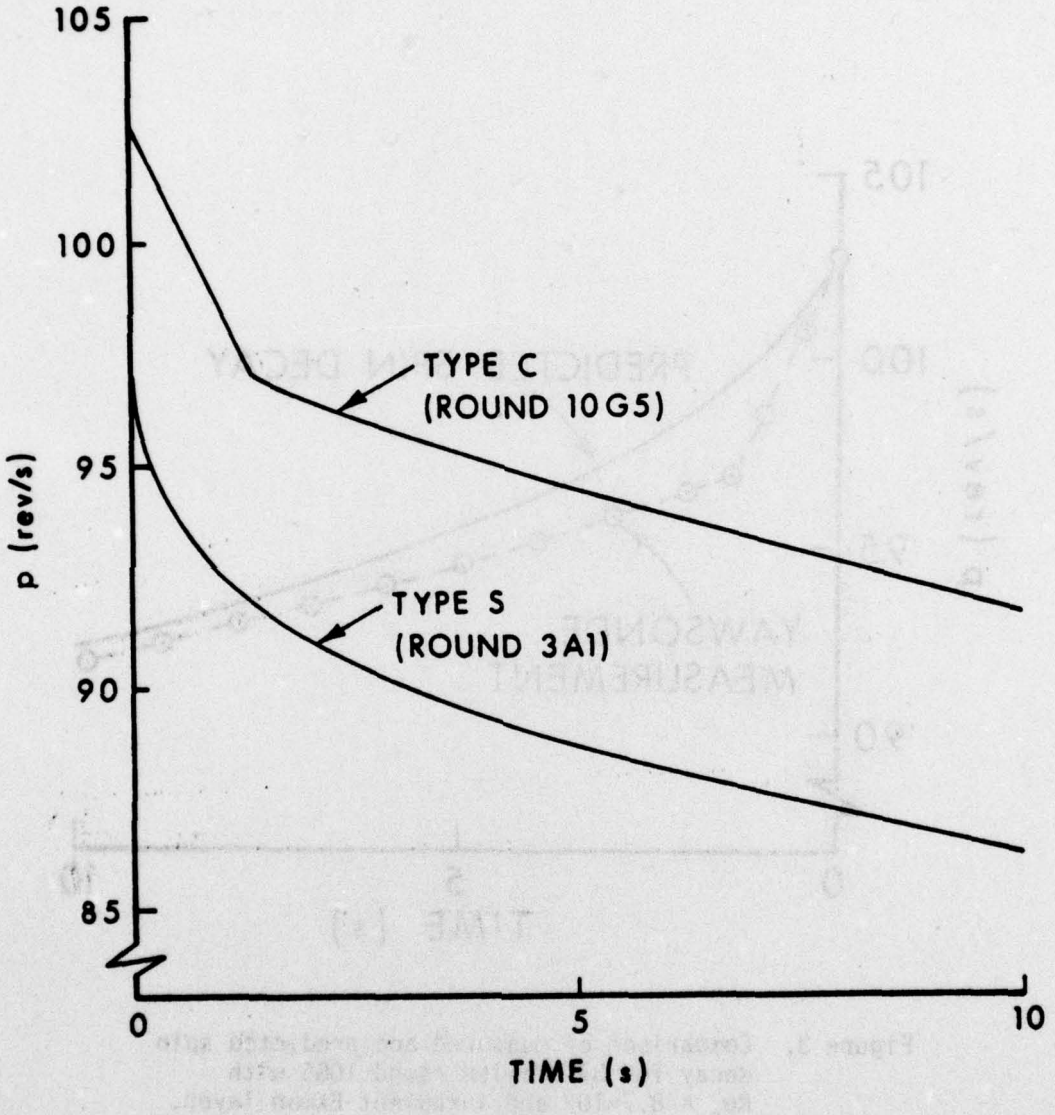

Figure 2. Two types of spin decay observed in firings of the XM687 shell.

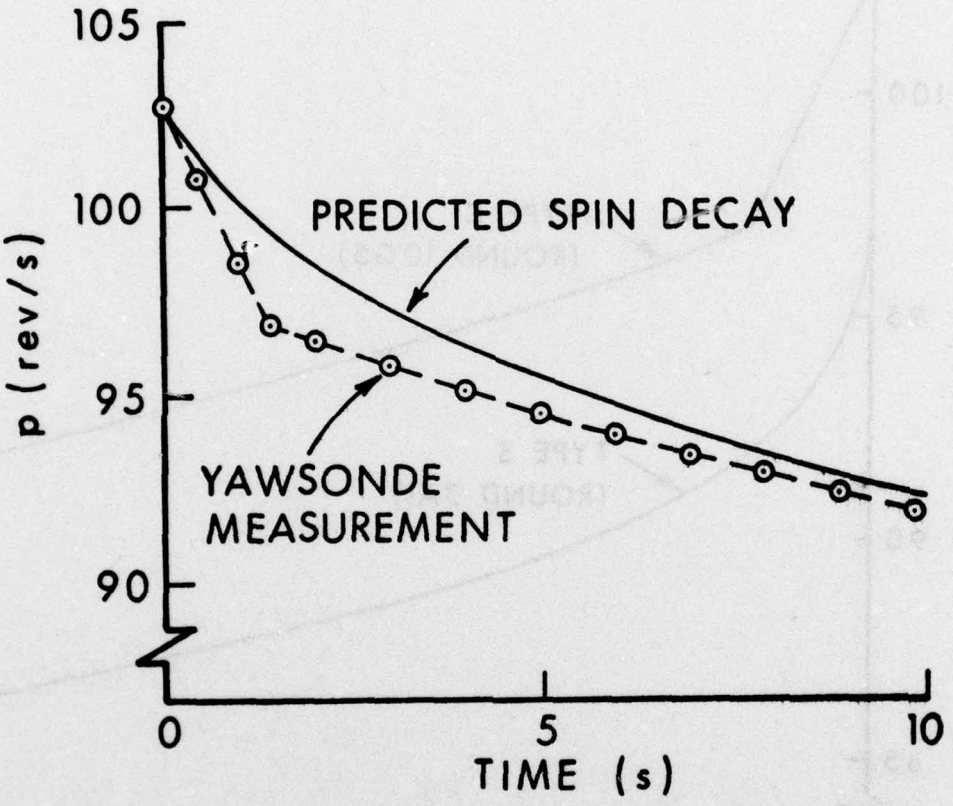

Figure 3. Comparison of measured and predicted spin decay for 87%-filled round 10G5 with $Re_o = 8.7 \times 10^5$ and turbulent Ekman layer.

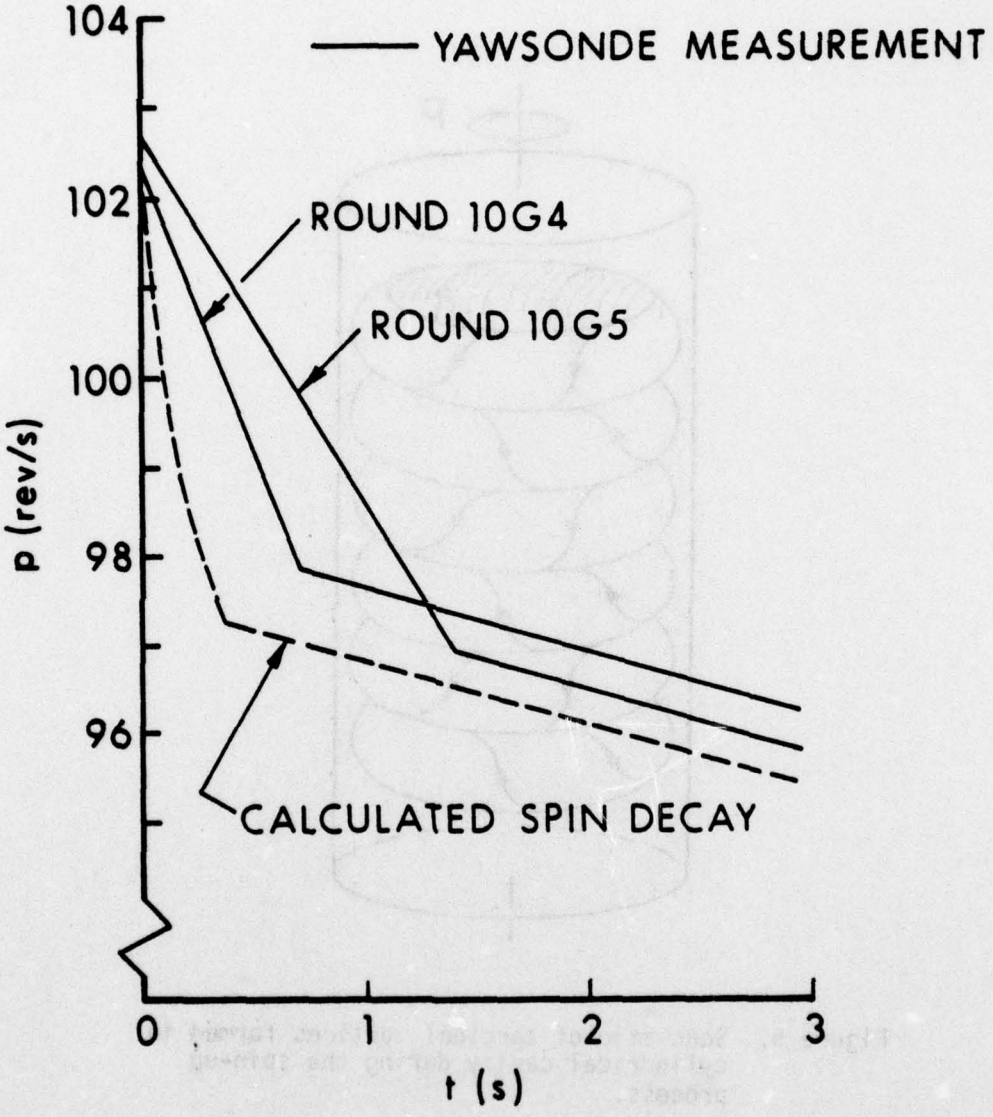

Figure 4. Comparison of measured spin decay for rounds 10G4 and 10G5 with that predicted assuming turbulent flow near the sidewall.

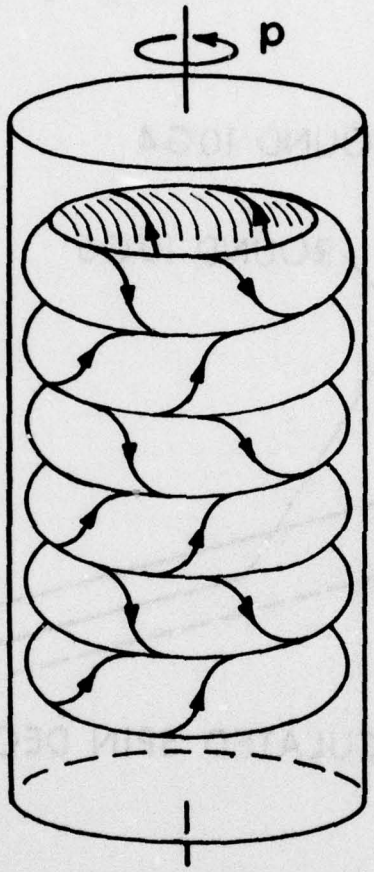

Figure 5. Schematic of toroidal vortices formed in cylindrical cavity during the spin-up process.

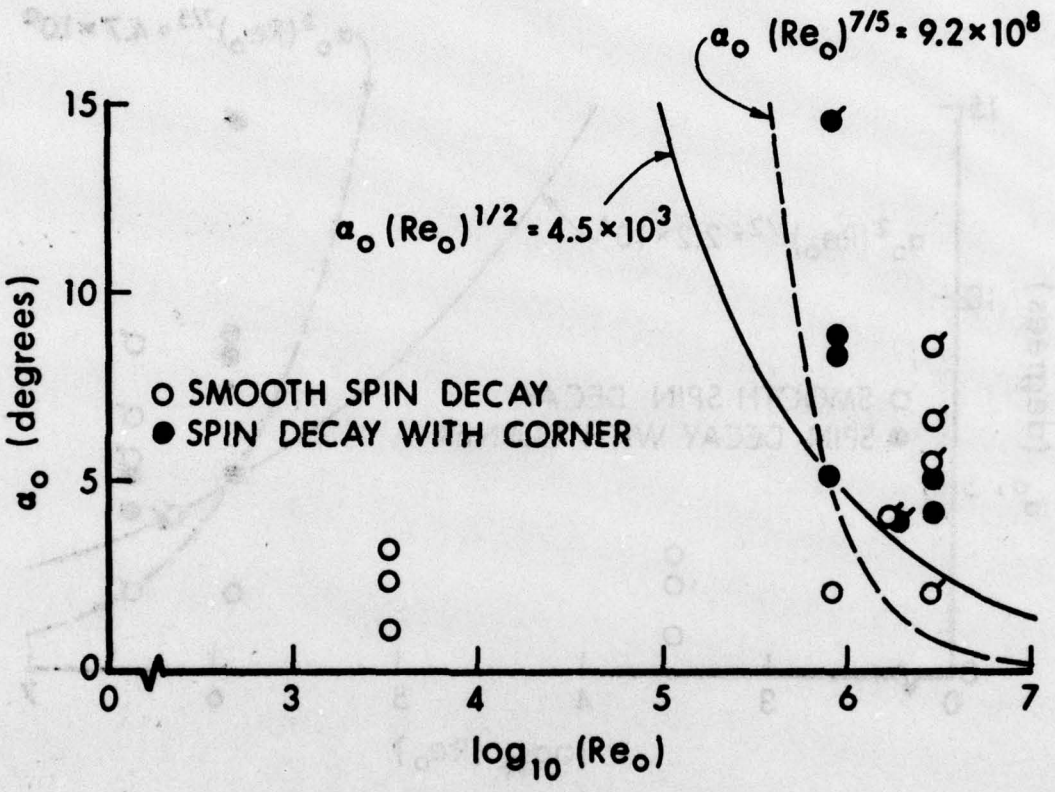

Figure 6. Comparison of spin record type with $\alpha_0(Re_0)^{\frac{1}{2}}$ for laminar Ekman layer and $\alpha_0(Re_0)^{7/5}$ for turbulent Ekman layer.

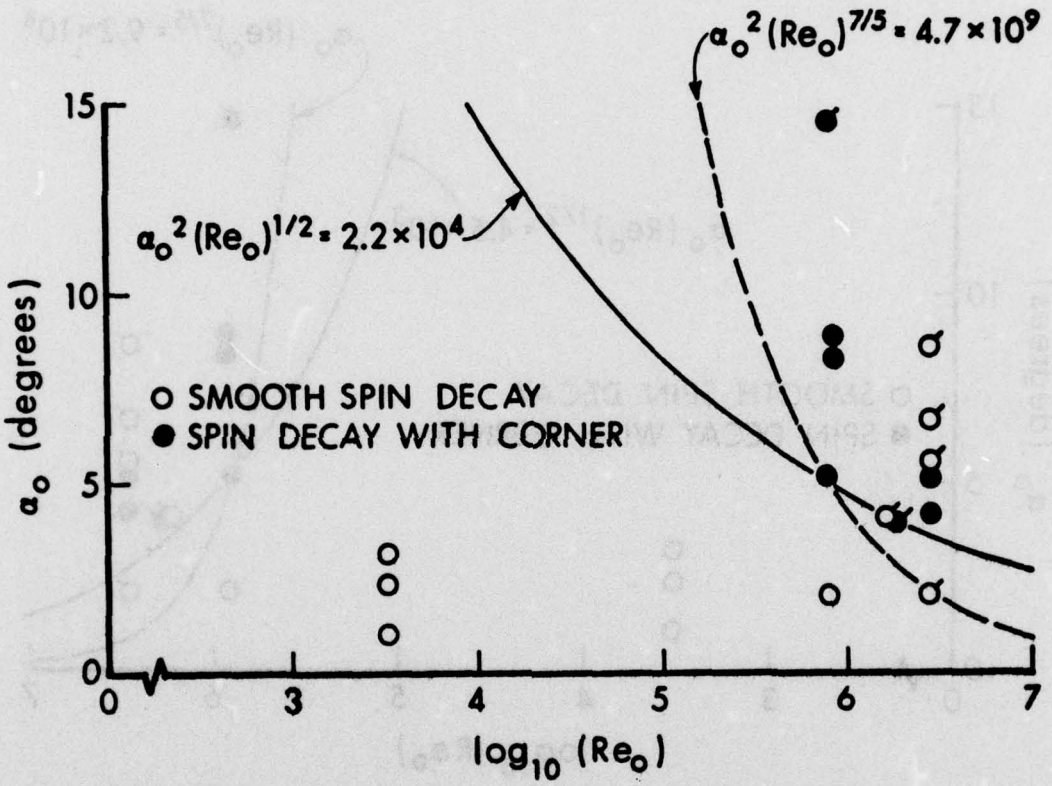

Figure 7. Comparison of spin record type with $(\alpha_o)^2 (Re_o)^{\frac{1}{2}}$ for laminar Ekman layer and $(\alpha_o)^2 (Re_o)^{7/5}$ for turbulent Ekman layer.

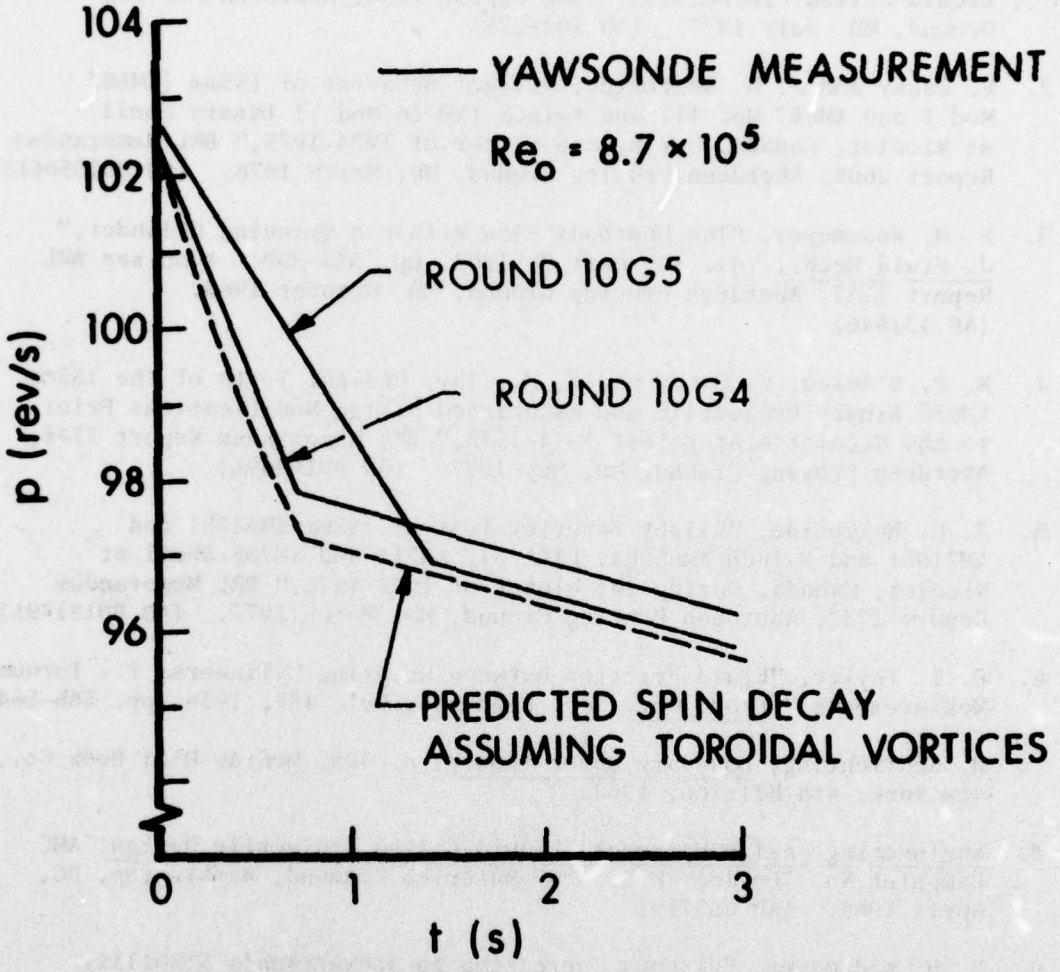

Figure 8. Comparison of measured spin decay for rounds 10G4 and 10G5 with that predicted from the flow model.

REFERENCES

1. C. W. Kitchens, Jr., and N. Gerber, "Prediction of Spin-Decay of Liquid-Filled Projectiles," BRL Report 1996, Aberdeen Proving Ground, MD, July 1977. (AD A043275)

2. V. Oskay and J. H. Whiteside, "Flight Behavior of 155mm (XM687 Mod I and XM687 Mod II) and 8-Inch (XM736 Mod I) Binary Shell at Nicolet, Canada, During the Winter of 1974-1975," BRL Memorandum Report 2608, Aberdeen Proving Ground, MD, March 1976. (AD B010566L)

3. E. H. Wedemeyer, "The Unsteady Flow Within a Spinning Cylinder," J. Fluid Mech., Vol. 10, Part 3, 1964, pp. 383-399. Also see BRL Report 1252, Aberdeen Proving Ground, MD, October 1963. (AD 431846)

4. W. P. D'Amico, V. Oskay and W. H. Clay, "Flight Tests of the 155mm XM687 Binary Projectile and Associated Design Modifications Prior to the Nicolet Winter Test 1974-1975," BRL Memorandum Report 2748, Aberdeen Proving Ground, MD, May 1977. (AD B019969L)

5. J. H. Whiteside, "Flight Behavior Test of 155mm XM687E1 and XM718E1 and 8-Inch XM650E4, PXR6231, XM711 and XM736 Shell at Nicolet, Canada, During the Winter of 1975-1976," BRL Memorandum Report 2732, Aberdeen Proving Ground, MD, March 1977. (AD B018149L)

6. G. I. Taylor, "Fluid Friction between Rotating Cylinders, I - Torque Measurements," Proc. Roy. Soc. London A, Vol. 157, 1936, pp. 546-564.

7. H. Schlichting, Boundary Layer Theory, p. 428, McGraw-Hill Book Co., New York, 4th Edition, 1960.

8. Engineering Design Handbook, Liquid-Filled Projectile Design, AMC Pamphlet No. 706-165, U.S. Army Materiel Command, Washington, DC, April 1969. (AD 853719)

9. E. H. Wedemeyer, "Viscous Correction to Stewartson's Stability Criterion," BRL Report 1325, Aberdeen Proving Ground, MD, June 1966. (AD 489687)

10. C. W. Kitchens, Jr., N. Gerber and R. Sedney, "Calculation of Liquid Eigenfrequencies and Decay Rates during Spin-Up in a Cylinder," BRL Report (in preparation).

11. F. H. Busse, "Steady Fluid Flow in a Precessing Spheroidal Shell," J. Fluid Mech., Vol. 33, Part 4, 1968, pp. 739-751.

12. Private communication from Dr. W. E. Scott, Launch and Flight Division, Ballistic Research Laboratory, June 1977.

REFERENCES (continued)

13. R. J. Donnelly and N. J. Simon, "An Empirical Torque Relation for Supercritical Flow Between Rotating Cylinders," J. Fluid Mech., Vol. 7, Part 3, 1960, pp. 401-418.

14. A. Mark, "Measurement of Angular Momentum Transfer in Liquid-Filled Shell," BRL Report (in preparation).

APPENDIX A

Summary of XM687 Firing Records

Five tables are presented to summarize the XM687 firing records that were examined in an attempt to correlate the spin record type (smooth or corner) with the launch parameters. This correlation is discussed in Section III. The tabulated data indicate: the round number; whether the launch was normal (N) or yaw was induced (IY); the fill ratio, β; whether the spin record shows smooth spin decay (S) or spin decay with a corner (C); the first maximum yaw angle, α_o; and the muzzle velocity, V_o. The solar angle and spin history for each round are presented in Reference 2, 4, 5 or 14; the appropriate reference is cited at the end of each table.

There is uncertainty about the spin record type and/or α_o for many of the rounds. Comments are used in these cases to explain why definite conclusions cannot be drawn. The indicated values of V_o in Table A1 are obtained from smear cameras located approximately 23m ahead of the muzzle; they are obtained from radar chronographs in Tables A2-A5. Except for the rounds in Table A4, the projectiles have the dual canister configuration depicted in Figure 1. The rounds in Table A4 were modified to have a single cylindrical cavity with dimensions approximately equal to those in the dual canister configuration after rupture of the discs.

---

14. *A. Mark, "Measurement of Angular Momentum Transfer in Liquid-Filled Shell," BRL Report (in preparation).*

PRECEDING PAGE BLANK-NOT FILMED

Table A1. XM687 Tested at Wallops Island in August 1974

Round	Launch	β	Record Type	α_o	V_o(m/s)	Comments
7168	IY	*	S (?)	5.5°	343.2	Spin record doesn't agree with stated V_o. Record is probably S-Type, but 0.5s of data is missing and it is difficult to tell.
7171	IY	*	No yawsonde data		326.1	
7178	IY	*	S (?)	6.6°	334.7	Spin record has unusually rapid initial decay.
7182	IY	*	C	4.1°	343.5	Radar extrapolation indicates V_o = 349.2 and this agrees with spin record.
7253	IY	*	C	5.1°	329.2	Radar extrapolation indicates V_o = 352.4.
7254	IY	*	?	9.1°	329.8	Spin record shows step decrease in spin at 1.06s. May signal lock-up of canister or liner. Drastic spin drop off at 6.3s as yaw amplifies.
7255	IY	*	?	3.0°	345.6	Radar extrapolation indicates V_o = 352.0. Spin record is unusual because first 0.87s shows linear decay and then it smoothly changes to aerodynamic decay. Type record uncertain.

All rounds have two canisters keyed to shell, containing a mixture of Freon 113 and ethyl alcohol ($\nu = 6.9\times10^{-7}$ m^2/s at 25°C). The solar angle and spin histories for these rounds are presented in Reference 4.

* The fill ratio is not accurately known, but it is expected to be approximately 0.9.

Table A2. XM687 Tested at Yuma Proving Ground in September 1974

Round	Launch	β	Record Type	α_o	V_o(m/s)	Comments
3636	IY	*	?	8.9°	330.4	Spin record indicates p_o > 108 which is inconsistent with stated V_o. If corner occurs it is less than 0.54s into flight.
3637	IY	*	Not enough data to tell		337.7	
3638	IY	*	Not enough data to tell		337.7	
3639	IY	*	S (?)	8.5°	333.5	If corner occurs it is less than 0.48s into flight. Spin record p_o is consistent with stated V_o if record is assumed to be Type S.
3644	N	*	S (?)	2°	337.7	If corner occurs it is less than 1.0s into flight. Spin record p_o is consistent with stated V_o if record is assumed to be Type S.

All rounds have two canisters keyed to shell, containing a mixture of Freon 113 and ethyl alcohol ($\nu = 6.9\times10^{-7}$ m^2/s at 25°C). The solar angle and spin histories for these rounds are presented in Reference 4.

* The fill ratio is not accurately known, but it is expected to be approximately 0.9.

Table A3. XM687 Tested at Nicolet in 1974-1975 Winter Tests

Round	Launch	β	Record Type	α_o	V_o(m/s)	Comments
10F1	IY	0.87	?	11.2°	327.5	Cannot decide type because of large nutation on spin record.
10F2	IY	0.87	?	8.1°	312.3	Cannot decide type because of large nutation on spin record.
10G1	IY	0.87	?	6.8°	285.7	Not enough data to tell. If corner occurs it is < 1.5 sec into flight.
10G2	IY	0.87	?	10.5°	281.3	Cannot decide type because of large nutation on spin record.
10G3	IY	0.87	?	10.5°	280.7	Cannot decide type because of large nutation on spin record.
10G4	IY	0.87	C	8.3°	313.2	
10G5	IY	0.87	C	8.8°	314.3	

All rounds have two canisters keyed to shell, containing a mixture of Freon 113 and ethyl alcohol ($\nu = 2.1\times10^{-6}$ m^2/s at 0°C). The solar angle and spin histories for these rounds are presented in Reference 2.

Table A4. XM687 Tested at Wallops Island in June 1975

Round	Launch	β	Record Type	α_o	V_o(m/s)	Payload	Comments
7450	N	1.00	No data near muzzle		292.8	O	
7670	N	1.00	S	2.3°	284.7	O	
7672	N	0.90	S	?	284.5	W	
7673	N	0.90	S	3.1°	292.9	O	
7675	N	1.00	No data near muzzle		289.8	W	
7676	N	0.90	S	4° (?)	291.8	W	Too much noise for accurate first max. yaw measurement.
7677	N	0.90	S	1°	293.4	O	
7678	N	0.80	S	3.0°	292.5	W	Foam end pads used with liquid payload.
7679	N	0.80	S	?	296.3	W	Foam end pads used with liquid payload.

All rounds have canister keyed to shell. There is only a single canister in each shell. Payload is indicated by either O - oil ($\nu = 5.0\times10^{-4}$ m^2/s) or W - water ($\nu = 1.0\times10^{-6}$ m^2/s). The solar angle and spin histories for these rounds are presented in Reference 14.

Table A5. XM687 Tested at Nicolet in 1975-1976 Winter Tests

Round	Launch	β	Round Type	α_o	V_o(m/s)	Comments
3A1	N	0.87	S	2°	295.4	
3B1	IY	0.87	?	11° (?)	300.2	Not enough data to tell. If corner occurs it is < .3 sec into flight.
3B2	IY	0.87	C (?)	14.5°	294.3	It is difficult to decide type because of large nutation on spin record.
3B3	IY	0.87	?	12°	292.5	Not enough data to tell. If corner occurs it is < .9 sec into flight.
3B4	IY	0.87	?	11°	292.5	Not enough data to tell. If corner occurs it is < .6 sec into flight. Based on muzzle velocity stated, spin at muzzle is 94.8 which is lower than indicated on spin record. Canister not keyed.
3B5	IY	0.87	S (?)	11.5°	293.2	Based on muzzle velocity stated, spin at muzzle is 95.1 which is lower than indicated by spin record. Canister not keyed.
3C1	IY	0.87	?	12° (?)	300.6	Not enough data to tell. If corner occurs it is < 2 sec into flight.
4A1	N	0.87	C	5.1°	286.2	
4B1	N	0.87	No data near muzzle		287.3	Canister not keyed.
4B2	N	0.87	No data near muzzle		283.8	Canister not keyed.

Table A5. XM687 Tested at Nicolet in 1975-1976 Winter Tests (continued)

Round	Launch	β	Round Type	α_o	V_o(m/s)	Comments
5B1	N	0.87	C (?)	4°	661.0	It is difficult to be certain of type.
5B2	N	0.87	C (?)	?	661.7	It is difficult to be certain of type.
5B3	N	0.87	No data near muzzle		661.2	
5B4	N	0.87	No data near muzzle		662.3	
5B5	N	0.87	C (?)	?	663.6	It is difficult to be certain of type.

All rounds except 3B4, 3B5, 4B1 or 4B2 have canisters keyed to shell. All rounds have two canisters containing a mixture of Freon 113 and ethyl alcohol ($\nu = 2.1\times10^{-6}$ m^2/s at 0°C). The solar angle and spin histories for these rounds are presented in Reference 5.

LIST OF SYMBOLS

a	radius of shell cylindrical cavity (m)
c	half-height of shell cylindrical cavity (m)
d	thickness of perturbation boundary layer (m)
$f(t)$	defined by Eq. (5) for rounds 10G4 and 10G5 (kg-m^2/s)
k_ℓ	laminar Ekman layer parameter defined by Eq. (10) (nondimensional)
k_t	turbulent Ekman layer parameter defined by Eq. (3) (nondimensional)
p	instantaneous spin rate of shell (s^{-1})
p_c	shell spin rate when the liquid reaches solid-body rotation (s^{-1})
p_o	shell spin rate at muzzle (s^{-1})
t	time measured from instant of projectile release from gun tube (s)
t_c	time when $p = p_c$ as calculated from Eq. (1) (s)
C	designates spin record type with corner (no associated units)
C_1-C_8	constants in Eqs. (6), (8) and (11) - (16) (nondimensional)
C_{ℓ_p}	projectile roll damping coefficient (nondimensional)
D	instantaneous distance from the sidewall to the inviscid front in the Wedemeyer spin-up model (m)
I_z	axial moment of inertia of projectile casing (kg-m^2)
K	constant of proportionality in Eq. (17) (nondimensional)
L	liquid angular momentum (kg-m^2/s)
M	projectile Mach number (nondimensional)
M_{Aero}	aerodynamic moment acting on shell due to air shear (N-m)

PRECEDING PAGE BLANK-NOT FILMED

LIST OF SYMBOLS (continued)

M_{Liq}	liquid moment acting on shell due to shear stress at cavity walls (N-m)
Re_o	launch Reynolds number of shell ($= p_o a^2/\nu$) (nondimensional)
S	designates spin record type that is smooth (no associated units)
$\overline{S}$	gap width between two concentric cylinders (m)
ΔV	change in liquid tangential velocity across the gap between two concentric cylinders (m/s)
α	projectile yaw angle (degrees)
α_o	first maximum yaw angle (degrees)
β	fill ratio; ratio of liquid volume to total cavity volume (nondimensional)
ν	kinematic viscosity of liquid (m^2/s)
ρ	liquid payload density (kg/m^3)

DISTRIBUTION LIST

No. of Copies	Organization
12	Commander Defense Documentation Center ATTN: DDC-TCA Cameron Station Alexandria, VA 22314
1	Commander US Army Materiel Development and Readiness Command ATTN: DRCDMA-ST 5001 Eisenhower Avenue Alexandria, VA 22333
1	Commander US Army Aviation Research and Development Command ATTN: DRSAV-E 12th and Spruce Streets St. Louis, MO 63166
2	Commander US Army Air Mobility Research and Development Laboratory ATTN: SAVDL-D W. J. McCroskey Ames Research Center Moffett Field, CA 94035
1	Commander US Army Electronics Command ATTN: DRSEL-RD Fort Monmouth, NJ 07703
1	Commander US Army Jefferson Proving Gd ATTN: STEJP-TD-D Madison, IN 47250
3	Commander US Army Missile Research & Development Command ATTN: DRDMI-TD Ray Deep DRDMI-R Redstone Arsenal, AL 35809
1	Commander US Army Tank Automotive Development Command ATTN: DRDTA-RWL Warren, MI 48090
1	Commander US Army Armament Materiel Readiness Command Rock Island, IL 61202
1	Commander US Army Armament Research & Development Command ATTN: DRDAR-LCA-F, A. Loeb Dover, NJ 07801
1	Commander US Army Harry Diamond Labs ATTN: DRXDO-TI 2800 Powder Mill Road Adelphia, MD 20783
1	Director US Army TRADOC SYSTEMS Analysis Activity ATTN: ATAA-SL (Tech Lib) White Sands Missile Range NM 88002
1	Commander US Army Research Office ATTN: R. E. Singleton P. O. Box 12211 Research Triangle Park NC 27709
1	Commander US Army Waterways Experiment Station ATTN: R. H. Malter Vicksburg, MS 39180

DISTRIBUTION LIST

No. of Copies	Organization
1	AGARD-NATO ATTN: R. H. Korkegi APO New York 09777
3	Commander US Naval Air Systems Command ATTN: AIR-604 Washington, DC 20360
3	Commander US Naval Ordnance Systems Command ATTN: ORD-0632 ORD-035 ORD-5524 Washington, DC 20360
2	Commander David W. Taylor Naval Ship Research & Development Command ATTN: H. J. Lugt, Code 1802 S. de los Santos Head, High Speed Aero Div Bethesda, MD 20084
6	Commander US Naval Surface Weapons Center Applied Aerodynamics Division ATTN: K. R. Enkenhus M. Ciment R. Lee S. M. Hastings A. E. Winklemann W. C. Ragsdale Silver Spring, MD 20910
1	Commander US Naval Surface Weapons Ctr ATTN: Tech Library Dahlgren, VA 22448
1	AFATL (DLDL, Dr. D. C. Daniel) Eglin AFB, FL 32542
2	AFFDL (W. L. Hankey; J. S. Shang) Wright-Patterson AFB, OH 45433
7	Director National Aeronautics and Space Administration ATTN: F. R. Bailey D. R. Chapman J. Marvin J. D. Murphy J. Rakich W. C. Rose B. Wick Ames Research Center Moffett Field, CA 94035
6	Director National Aeronautics and Space Administration Langley Research Center ATTN: J. E. Carter J. E. Harris E. Price J. South J. R. Sterrett Tech Library Langley Station Hampton, VA 23365
1	Director National Aeronautics and Space Space Administration Lewis Research Center ATTN: MS 60-3, Tech Lib 21000 Brookpark Road Cleveland, OH 44135
1	Director National Aeronautics and Space Administration Marshall Space Flight Center ATTN: A. R. Felix, Chief S&E-AERO-AE Huntsville, AL 35812

DISTRIBUTION LIST

No. of Copies	Organization
2	Director Jet Propulsion Laboratory ATTN: J. Kendall Tech Lib 4800 Oak Grove Drive Pasadena, CA 91103
3	ARO, Inc. ATTN: J. D. Whitfield R. K. Matthews J. C. Adams, Jr. Arnold AFB, TN 37389
3	Aerospace Corporation ATTN: T. D. Taylor H. Mirels R. L. Varwig Aerophysics Lab P. O. Box 92957 Los Angeles, CA 90009
1	AVCO Systems Division ATTN: B. Reeves 201 Lowell Street Wilmington, MA 01887
3	The Boeing Company Commercial Airplane Group ATTN: W. A. Bissell, Jr. M. S. 1W-82, Org 6-8340 P. E. Rubbert J. D. McLean Seattle, WA 98124
2	Calspan Corporation ATTN: A. Ritter M. S. Holden P. O. Box 235 Buffalo, NY 14221
1	Center for Interdisciplinary Programs ATTN: Victor Zakkay W. 177th St. & Harlem River Bronx, NY 10453
1	General Dynamics ATTN: Research Lib 2246 P. O. Box 748 Fort Worth, TX 76101
1	General Electric Company ATTN: H. T. Nagamatsu Research & Development Lab (Comb. Bldg.) Schenectady, NY 12301
1	General Electric Co., RESD ATTN: R. A. Larmour 3198 Chestnut Street Philadelphia, PA 19101
3	Grumman Aerospace Corporation ATTN: R. E. Melnik L. G. Kaufman B. Grossman Research Department Bethpage, NY 11714
2	Lockheed-Georgia Company ATTN: B. H. Little, Jr. G. A. Pounds Dept 72074, Zone 403 86 South Cobb Drive Marietta, GA 30062
1	Lockheed Missiles & Space Co. ATTN: Tech Info Center 3251 Hanover Street Palo Alto, CA 94304
4	Martin-Marietta Laboratories ATTN: S. H. Maslen S. C. Traugott K. C. Wang H. Obremski 1450 S. Rolling Road Baltimore, MD 21227

DISTRIBUTION LIST

No. of Copies	Organization
2	McDonnell Douglas Astronautics Corporation ATTN: J. Xerikos H. Tang 5301 Bolsa Avenue Huntington Beach, CA 92647
1	McDonnell-Douglas Corporation Douglas Aircraft Company ATTN: T. Cebeci 3855 Lakewood Boulevard Long Beach, CA 90801
1	Northrup Corporation Aircraft Division ATTN: S. Powers 3901 West Broadway Hawthorne, CA 90250
2	Sandia Laboratories ATTN: F. G. Blottner Tech Lab Albuquerque, NM 87115
2	United Aircraft Corporation Research Laboratories ATTN: R. W. Briley Library East Hartford, CT 06108
1	Vought Systems Division LTV Aerospace Corporation ATTN: J. M. Cooksey Chief, Gas Dynamics Lab., 2-53700 P. O. Box 5907 Dallas, TX 75222
1	California Institute of Technology Guggenheim Aeronautical Lab ATTN: Tech Lib Pasadena, CA 91104
2	California Institute of Technology ATTN: H. B. Keller Mathematics Dept. D. Coles Aeronautics Dept. Pasadena, CA 91109
1	Cornell University Graduate School of Aero Engr ATTN: Library Ithaca, NY 14850
2	Illinois Institute of Tech ATTN: M. V. Morkovin H. M. Nagib 3300 South Federal Chicago, IL 60616
1	The Johns Hopkins University ATTN: S. H. Davis Dept of Mechanics & Materials Science Baltimore, MD 21218
2	Massachusetts Institute of Technology ATTN: E. Covert Tech Library 77 Massachusetts Avenue Cambridge, MA 02139
2	North Carolina State University Mechanical and Aerospace Engineering Department ATTN: F. F. DeJarnette J. C. Williams Raleigh, NC 27607

DISTRIBUTION LIST

No. of Copies	Organization
1	Notre Dame University ATTN: T. J. Mueller Dept. of Aero Engr South Bend, IN 46556
2	Ohio State University Dept. of Aeronautical and Astronautical Engineering ATTN: S. L. Petrie O. R. Burggraf Columbus, OH 43210
2	Polytechnic Institute of New York ATTN: G. Moretti S. G. Rubin Route 110 Farmingdale, NY 11735
1	Princeton University Dept. of Aerospace and Mechanical Sciences ATTN: S. I. Cheng Princeton, NJ 08540
3	Princeton University James Forrestal Research Center Gas Dynamics Laboratory ATTN: I. E. Vas S. M. Bogdonoff Tech Lib Princeton, NJ 08540
1	Purdue University Thermal Science & Prop Center ATTN: D. E. Abbott W. Lafayette, IN 47907
1	Rensselaer Polytechnic Institute Dept. of Math. Sciences ATTN: R. C. DiPrima Troy, NY 12181
1	Rutgers University Dept. of Mechanical, Industrial and Aerospace Engineering ATTN: R. H. Page New Brunswick, NJ 08903
1	Southern Methodist University Dept. of Civil & Mechanical Engineering ATTN: R. L. Simpson Dallas, TX 75275
1	Southwest Research Institute Applied Mechanics Reviews 8500 Culebra Road San Antonio, TX 78228
1	University of California - Berkley Dept. of Aerospace Engineering ATTN: M. Holt Berkeley, CA 94720
1	University of California - Davis ATTN: H. A. Dwyer Davis, CA 95616
2	University of California - San Diego Dept. of Aerospace Engineering & Mechanical Engr Sciences ATTN: P. Libby Tech Lib La Jolla, CA 92037
2	University of Cincinnati Dept. of Aerospace Engineering ATTN: R. T. Davis M. J. Werle Cincinnati, OH 45221

DISTRIBUTION LIST

No. of Copies	Organization
1	University of Colorado Dept. of Astro-Geophysics ATTN: E. R. Benton Boulder, CO 80302
1	University of Hawaii Dept. of Ocean Engineering ATTN: G. Venezian Honolulu, HI 96822
2	University of Maryland ATTN: W. Melnik J. D. Anderson College Park, MD 20740
1	University of Michigan Department of Aeronautical Engineering ATTN: Tech Lib East Engineering Building Ann Arbor, MI 48104
1	University of Santa Clara Department of Physics ATTN: R. Greeley Santa Clara, CA 95053
3	University of Southern Cal. Dept. of Aerospace Engineering ATTN: T. Maxworthy P. Weidman M. Hafez Los Angeles, CA 90007
1	University of Texas Dept of Aerospace Engineering ATTN: J. C. Westkaemper Austin, TX 78712
1	University of Virginia Dept. of Aerospace Engineering & Engineering Physics ATTN: I. D. Jacobson Charlottesville, VA 22904
1	University of Washington Dept. of Mechanical Engineering ATTN: Tech Lib Seattle, WA 98195
2	Virginia Polytechnic Institute Dept. of Aerospace Engineering ATTN: G. R. Inger F. J. Pierce Blacksburg, VA 24061
	Aberdeen Proving Ground
	Marine Corps Ln Ofc Dir, USAMSAA
	Munitions Systems Division Bldg. 3330 ATTN: E. A. Jeffers W. C. Dee W. J. Pribyl APG-EA
	Armament Concepts Office Bldg. 3516 (DRDAR-ACW) ATTN: M. C. Miller APG-EA